Prediction of residual stresses in bridge roller bearings using Abaqus

Joseph M. Bushell and Dr Nawal K. Prinja

AMEC Nuclear, Booths Park, Chelford Road, Knutsford, Cheshire, WA16 8QZ

Abstract: *An analysis of bridge roller bearings was performed using Abaqus as part of a failure investigation. Finite element analyses were conducted to gain an understanding of the stresses caused during operation and explain the possible cause of failure. Models of the bearings were required to represent the contact between the roller and plates, daily movement of the load and the non-linear behaviour of the material. An important output was prediction of residual stresses along the contact area of the rollers, induced by repeated rolling as the bridge expands due to daily and seasonal temperature cycles.*

Linear kinematic and non-linear isotropic/kinematic models available in Abaqus were used to model the material behaviour, both of which predicted significant tensile stresses at the roller surface that did not match experimental observations. Further, this tensile residual stress remained when the bearing load was reduced below that required to induce plasticity. Surprisingly, the residual stresses remained even when purely elastic material was used and were found to steadily increase in magnitude with further cycling. The cause of these spurious stresses is believed to be due to numerical modelling of the material combined with incremental analysis in Abaqus.

A new finite-elastic, finite-plastic (Fe-Fp) material model recently developed by Abaqus was used successfully to reduce this stress. However, at the time the analysis was performed it was only available for use with isotropic hardening, and was therefore inappropriate for modelling situations involving cyclic plasticity where kinematic effects are important. Due to the need to simulate rolling contact, geometric nonlinearity (NLGEOM option) had to be used. Caution must therefore be exercised when performing nonlinear analyses involving cyclic plasticity with geometric nonlinearity.

Keywords: *Residual stress, roller bearings, Thelwall viaduct, NLGEOM, FeFp, material hardening, isotropic, kinematic, non-linear, cyclic loads, elastic, plastic, civil, transport, user subroutines*

1. Introduction

A failure investigation has recently been performed to provide an explanation of roller bearing failures on the Thelwall viaduct in the UK. These bearings were located along the deck of the bridge to permit thermal expansion of the bridge due to daily and seasonal temperature cycles without exerting excessive loads on the supporting structure. Although designed for a service life of 30+ years, within a period of 3 years following installation significant cracking was identified in both rollers and plates of numerous bearings along the bridge. Some 25% of bearings on the bridge were found to have failed in this manner, with many others showing indications of crack initiation.

In this investigation, Finite Element Analysis (FEA) was used in conjunction with other analytical methods and areas of expertise as a tool to gain an understanding of the bearing behaviour under typical daily loading cycles and to subsequently postulate the likely failure mechanism. High loading and the need to model changing roller-to-plate contact required the representation of cyclic plasticity and non-linear geometric behaviour.

A requirement of this work was the prediction of the residual stresses within the roller and plates resulting from cyclic loading of the roller and plate material as the bearing moved from side to side. The purpose of this aspect of the work was both to identify whether tensile residual stresses were present of a sufficient magnitude to support a failure mechanism of stress-corrosion cracking and as a validation of the FEA when compared against experimental measurements. As a litigation argument centred on an incorrect choice of material leading to failure by stress-corrosion cracking, the absence of significant tensile stress would alternatively support a failure by mechanical means (i.e. fatigue) independent of the choice of material.

This paper focuses solely on the use of Abaqus for the prediction of residual stresses within the roller and plates and the issues uncovered during this work. The purpose of this paper is to draw attention to the problems encountered when simulating cyclic plasticity over multiple cycles in a non-linear geometric analysis, and to provide advice to analysts who may perform similar work.

2. Modelling Approach

2.1 Model Construction

A 2D plane strain model of the bearing was created using Abaqus/CAE, representing a section of the bearing away from the ends, as shown in Figure 1. The model consists of a 120mm diameter roller held in contact with two plates, with a further base plate beneath the bearing. The bearing is compressed by a vertical load applied to the top plate which holds the roller in place. Horizontal translation of the loaded top plate causes the bearing to roll.

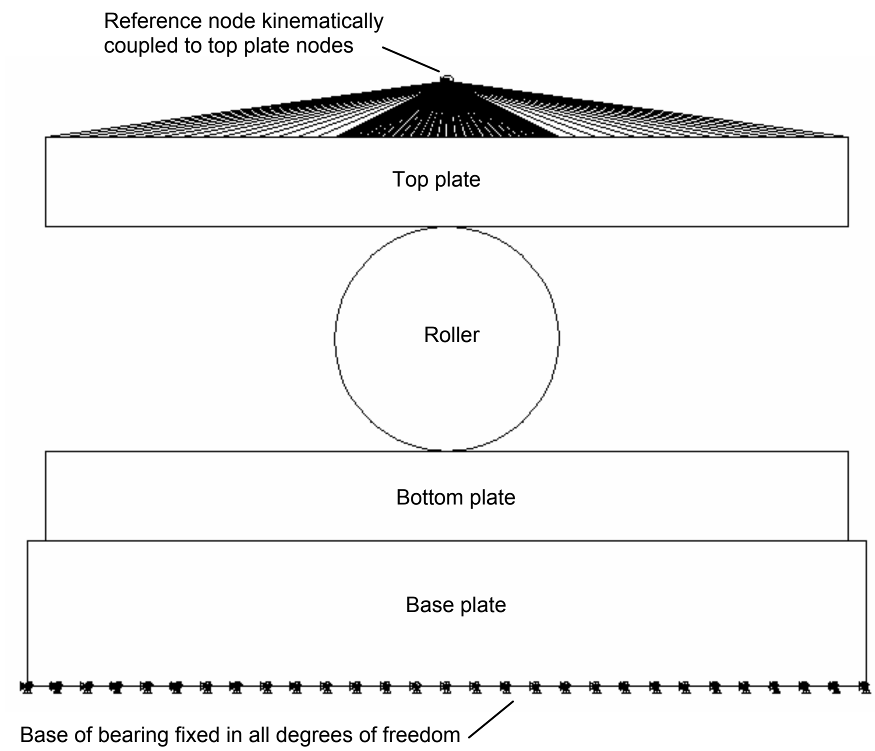

Figure 1. Layout of roller bearing and associated boundary conditions

A structured mesh was applied, with refinement in the contact regions towards the contact surfaces to capture the localised sub-surface stress concentrations typical in contact analyses. The elements applied are 4-noded bilinear plane-strain quadrilateral elements (Abaqus code CPE4). Plane strain elements were selected for the model to represent a mid-section of the roller, away from the ends. Linear elements have been used, as opposed to higher order elements, to effectively model contact at the roller and plate interfaces due to their favourable behaviour under uniform pressure. This is necessary as both the contact and frictional forces can vary strongly for higher order elements in contact depending on whether the mid-side nodes or the corner nodes are considered due to non-uniform equivalent nodal forces (Konter, 2000). However, the use of linear elements in a contact analysis requires the implementation of a much finer mesh, as shown in Figures 2 and 3, to obtain detailed resolution of the stresses at the contact interfaces. Sensitivity studies were performed to ensure that the mesh appropriately captured the sub-surface contact stresses.

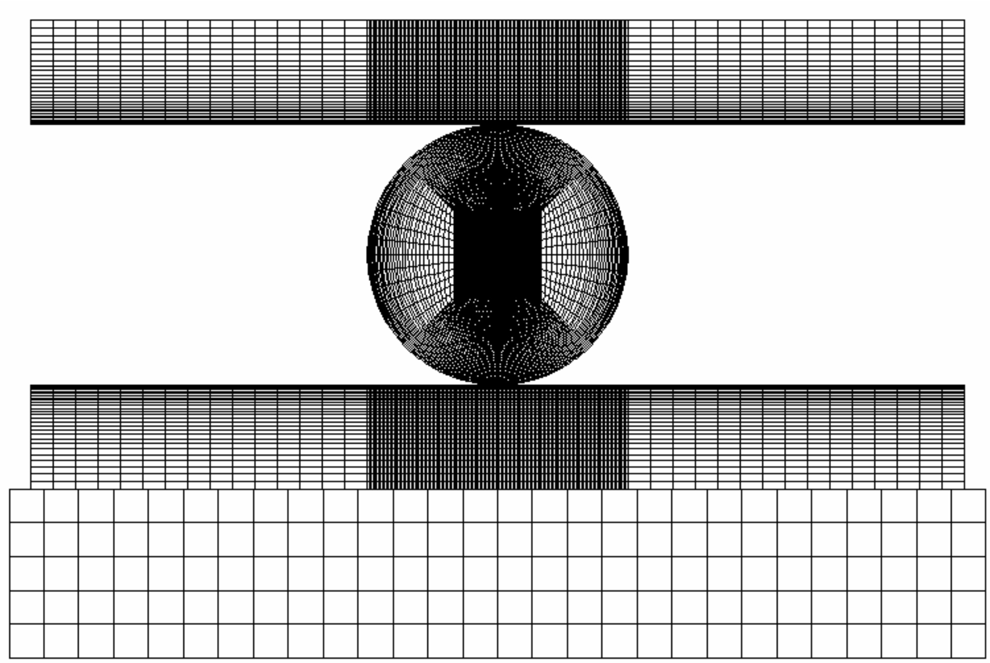

Figure 2. Model mesh

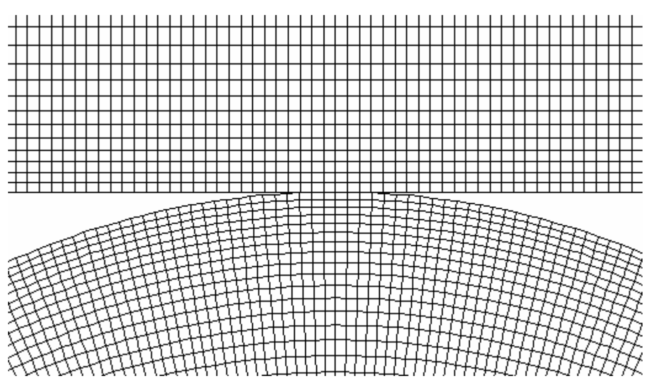

Figure 3. Mesh detail at contact interface

The units used in the analyses are Newtons (N) for Force, mm for dimensions and MPa (N/mm^2) for stress and pressure. The results presented for the roller consider a cylindrical stress system, where 1 is the radial direction, 2 is the hoop direction and 3 is the axial direction. When considering the plate, the default global system has been used, where 1 is the vertical direction, 2 is the horizontal direction and 3 is the out of plane direction.

2.2 Boundary Conditions

The lower surface of the base plate is constrained in the 1, 2 and 3-directions. The top roller plate degrees of freedom have been constrained to those of a reference node to keep the upper surface flat and to prevent the plate from bending over the roller as the load is applied. This is based upon the assumption that the bridge structure above the top plate is rigid and will not bow across the top of the bearing. Vertical loads and horizontal displacements are applied to this reference node and distributed to the nodes of the top plate upper surface. The roller itself is constrained purely by contact between the top and bottom roller plates.

2.3 Contact Interactions

A typical coefficient of friction (μ) of 0.25 for steel-steel contact has been applied for the contact between the roller and plates. However, sensitivity studies performed for different values of friction showed no appreciable difference in model behaviour, as under large vertical loads the roller will roll due to its geometry.

2.4 Material Properties

The roller material is stainless steel AISI 420 TQ+T, whereas the plate material is RAMAX S stainless holder steel. Table 1 summarises the key material properties applied for the roller and plates.

Material	**E (MPa)**	**ν**	**σ_y (MPa)**	**$RP_{0.2}$ (MPa)**	**R_m (MPa)**	**%A**
Roller	205500	0.3	1000	1385	1778	3%
Plate	200000	0.3	910	[not supplied]	1100	10%

Table 1. Summary of material parameters

where:

- E = Young's Modulus (MPa)
- ν = Poisson's Ratio
- σ_y = Yield Stress (MPa)
- $RP_{0.2}$ = Stress at offset strain of 0.2%
- Rm = Ultimate Tensile Stress (MPa)
- %A = Percentage elongation

Figure 4 shows the basic true stress-strain curves applied for each material.

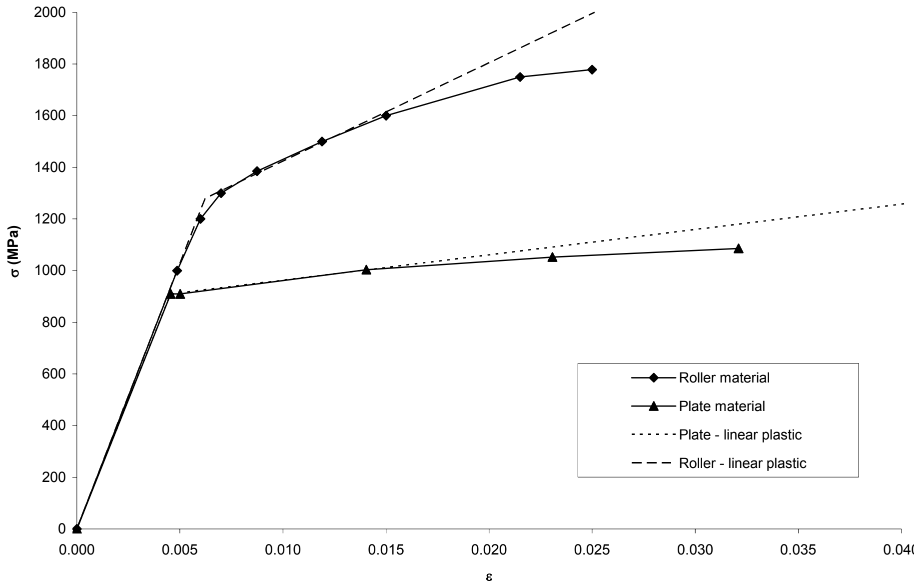

Figure 4. Stress-strain curves used for isotropic and linear kinematic analyses

Several material models were applied to the model:

- Isotropic (default)
- Linear kinematic
- Non-linear isotropic/kinematic

For load cycles involving cyclic plasticity, kinematic effects must be modeled to appropriately describe the Bauschinger effect. Initial analyses were performed using the basic data shown in Figure 4 for the isotropic and linear kinematic hardening models. The linear hardening slopes were chosen to coincide with the typical maximum strain magnitudes experienced by each material in the analysis.

The non-linear isotropic/kinematic model available in Abaqus for modeling cyclic plasticity of metals was used in later analyses following completion of displacement controlled tests of material samples at the typical strain ranges predicted by the initial FEA. This was considered the most realistic representation of the actual behaviour as it captures both isotropic and kinematic hardening properties of the material at the strain magnitudes considered. The input for this model was in the form of test data taken from a stabilized cycle.

2.5 Analysis Details

Analyses have been performed to reflect the loading conditions the bearing is expected to see during a typical day. The bearing is loaded with a design vertical load of 3924kN, corresponding to the maximum serviceability load state (SLS) load for each bearing, which includes factors of 1.2 on the superimposed load and 1.1 on the live load. Following initial application of the vertical load, the top plate undergoes a horizontal displacement of +/-27mm, based on an assumed typical thermal movement of 3.6mm/^{o}C for a typical daily temperature range of +/-7.5^{o}C. This corresponds to a distance of +/-13mm travel (12.89^{o} roll) seen by the roller as it rolls between the two plates. The analysis begins with an unloaded, undeformed roller aligned with the bearing principal axis. No temperature loadings have been applied in this analysis.

The analysis steps are illustrated in Figure 5.

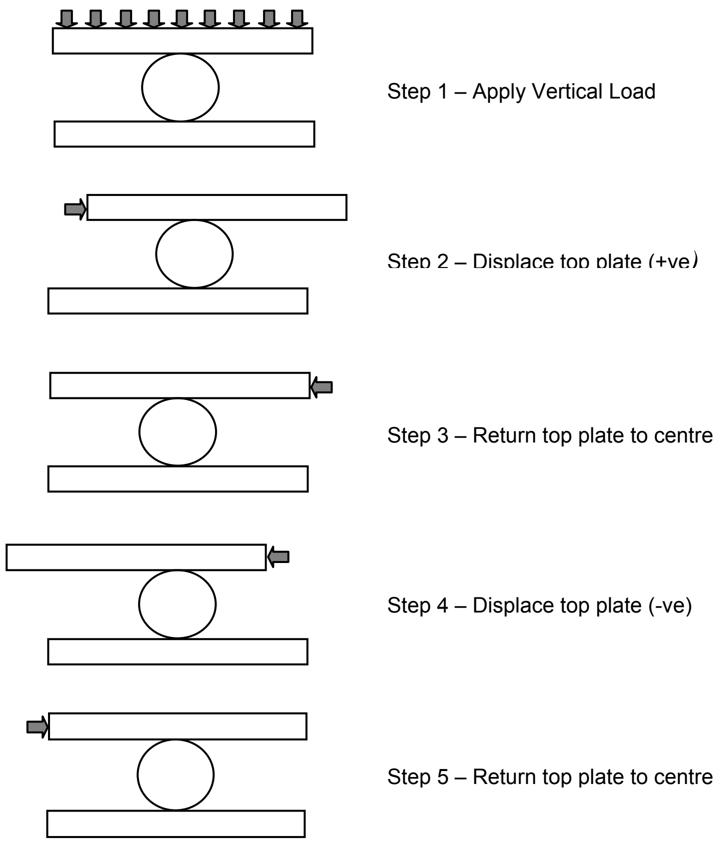

Figure 5. Analysis steps characterizing a typical daily load cycle

Steps 2 to 5 are repeated for 10 daily cycles under constant vertical load. This is considered sufficient for the material in the contact region to have reached a stable cyclic behaviour. The vertical load is subsequently removed to allow the remaining residual stresses to be determined.

The bearing model was analysed using Abaqus/Standard version 6.7-1. As during rolling the contact between the roller and plates changes, a non-linear geometric analysis (NLGEOM option) was required.

3. Analysis Results

3.1 Description of Stress System

In operation, the magnitude of load experienced is sufficient to cause plastic deformation and thereby induce residual stresses. In this particular analysis, the load is sufficient to cause continuous plastic deformation with each cycle. Figure 6 illustrates the stress system considered within the contact area.

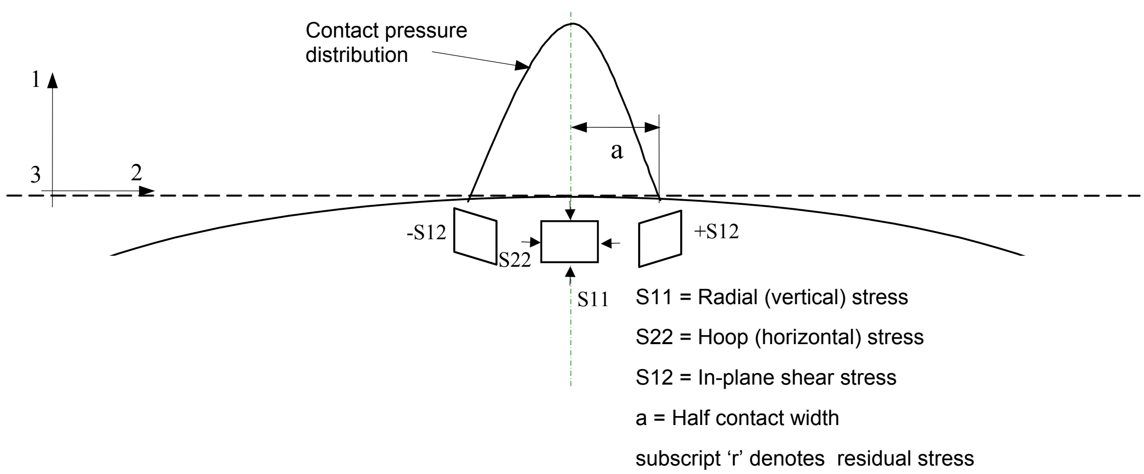

Figure 6. Stress system associated with contact area

Direct compressive stress acting on an element will compress and a direct tensile stress will elongate the element. Shear stress (S12) will distort the element by shearing it, i.e. one side moves relative to the other. The material directly at the centre of the contact patch is under pure compression in the vertical direction and in the hoop direction. Shear stresses in the vertical plane begin to develop away from the centre of the compressed region as the material adjusts between compressed and uncompressed regions. Yielding first occurs directly under the point of contact by compression followed by shearing between compressed material and less compressed material on either side.

Considering the residual stress distribution in the roller, the assumption of plane strain will eliminate out of plane residual shear stresses $(S13)_r$ and $(S23)_r$ and make the remaining components constant in the axial (3) direction. Away from the edges of the area traversed by the point of contact, plastic deformation can be assumed to be steady and continuous, such that the surface profile of the roller will not change, and therefore be considered constant in the hoop (2) direction. For the residual stresses to be in equilibrium with a traction free surface, residual stresses cannot exist in the radial (1) direction, eliminating $(S11)_r$ and $(S12)_r$. This means that the only possible residual stress system for the plane strain case involves hoop $(S22)_r$ and axial $(S33)_r$ residual stresses. The subject of this investigation is the hoop component of the residual stress. For free rolling contact, both components of residual stress will be compressive, with maximum values at the depth of maximum in plane shear stress, S12 (Johnson, 1989). This was found by both theory (Johnson, 1989) and the FEA results to occur at a depth of approximately 1.8mm below the contact surface.

3.2 Residual Stresses from 2D Bearing Analysis

Figure 7 shows the resulting residual hoop stress in the roller predicted by the FEA compared to the result obtained from experimental measurements, which were measured by MATTEC using the cut-compliance method (Schindler, 2005). This result is taken from a path running radially from the roller surface into the underlying material in the centre of the contact area on the roller.

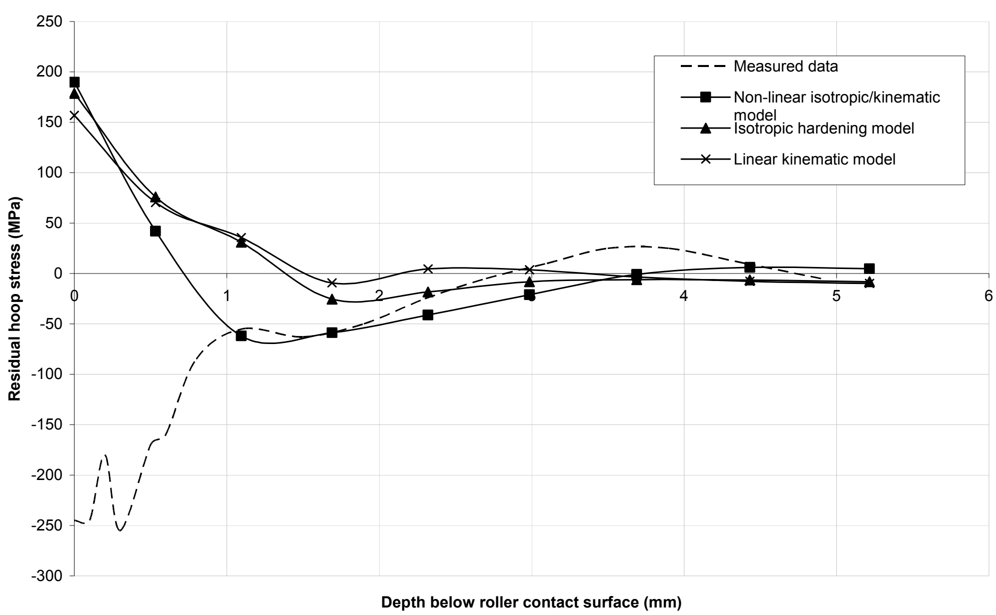

Figure 7. Residual hoop stress in the roller predicted by FEA compared to experimental measurements

Both the predicted and measured residual stress distributions exhibit a compressive hoop stress at approximately 1.8mm below the surface, which corresponds to the location of maximum sub-surface shear stress beneath the point of contact when the roller is loaded. The magnitude of this compressive stress is however small due to the small amount of plasticity in the roller caused by the applied load. The closest match to the measured data is exhibited by the non-linear isotropic/kinematic hardening model, which is expected as it is the most representative of the actual material behaviour. However, the near surface residual hoop stresses predicted by the FEA are tensile compared to with the measured stress which is compressive.

To investigate the cause of this tensile stress, the analysis was repeated for reduced vertical load. These results are shown in Figure 8.

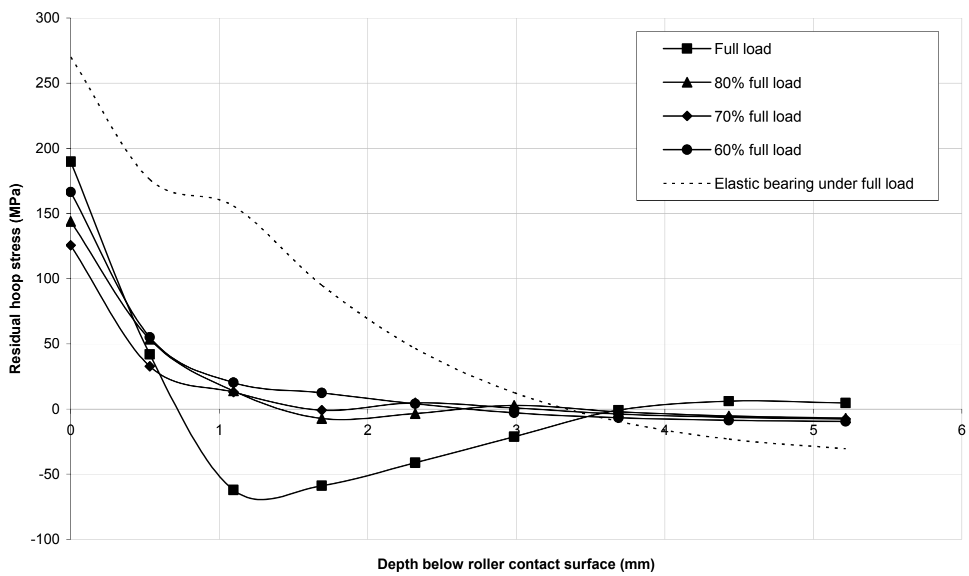

Figure 8. Effect of vertical load on residual hoop stress in the roller

It was found that, although the compressive residual stress reduces with reducing vertical load and resulting plasticity, the magnitude of the tensile stress remains largely unchanged. A further analysis was therefore performed for a purely elastic bearing under the full load, the results of which are also shown in Figure 8. The tensile residual hoop stress remained even with a purely elastic material! It is evident that this level of residual hoop stress in a purely elastic material is unrealistic and must therefore have been caused by numerical features / algorithms in Abaqus.

To explain this observation, reference can be made to Abaqus answer 1228. To summarise, this answer explains the presence of this ‘spurious’ stress as characteristic of the incremental solution approach taken when applying the *Elastic material model in a geometrically non-linear analysis (NLGEOM). In an NLGEOM analysis, an increment of strain is required for the constitutive calculations, which is derived by integration of the strain rate over the time of the increment.

However, in this case the reference condition for the integration of the strain rate is that of the model at the end of the previous increment, as opposed to the start of the analysis. This is known to lead to a non-zero strain, and therefore stress, in closed loop loading. The relationship with the size of time increment implies that reducing the increment size of the analysis will help to reduce this effect. It also suggests that the extent of this error will increase with number of cycles.

Although for small-strain analyses this strain is expected to remain very small compared to the overall results of the analysis, in the rolling contact case considered here it has been found to be significant compared to both the residual stress and the general magnitude of stress when the bearing is loaded (approximately 8-10% of the loaded stress). In addition, as the analysis deals with material hardening over multiple cycles, reducing the time increment can be impractical, particularly for a 3D analysis.

Figure 9 illustrates the effect of reducing the maximum time increment on the 'spurious' residual stress produced. In this case, the purely elastic bearing analysis has been processed using a maximum time increment of 0.01. This demonstrates a significant reduction in the magnitude of artificial stress generated when the analysis is forced to use small time increments.

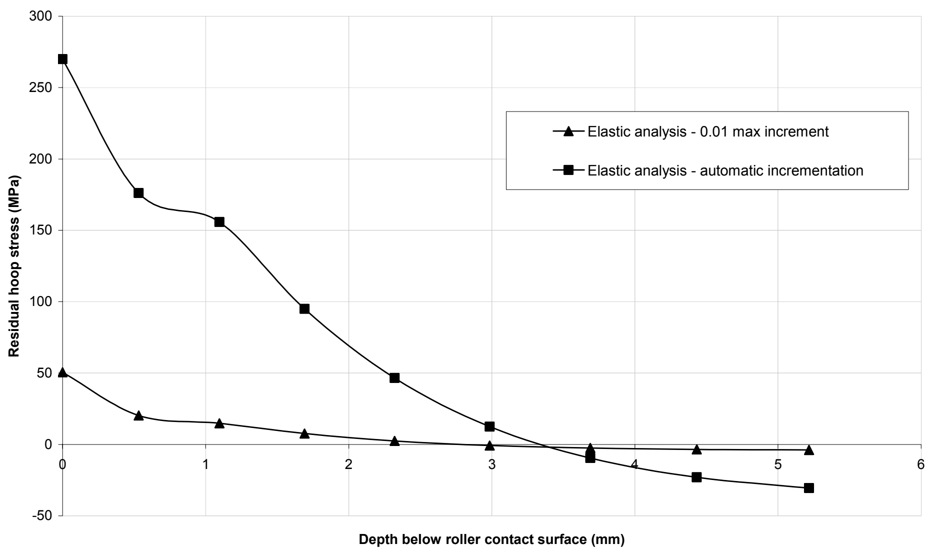

Figure 9. Effect of reducing the maximum time increment on the magnitude of 'spurious' stress generated

3.3 Simplified Analysis

In order to verify NLGEOM as the root cause of this spurious stress, a simplified representation of the roller-plate contact was developed, as shown in Figure 10. In this instance, the roller has been replaced by an equivalent moving Hertzian pressure distribution applied to the surface of the plate using the DLOAD user sub routine. This approach has been used for similar FEA for the prediction of residual stresses (Jiang, Chang and Xu, 2001, Jiang, Xu and Sehitoglu, 2002, Guo and Barkey, 2004) and, as it does not involve computation of contact conditions, a geometrically linear analysis may be performed. Given the majority of plastic deformation occurs in the first 1-2 cycles, this is a reasonable representation of the stable contact pressure.

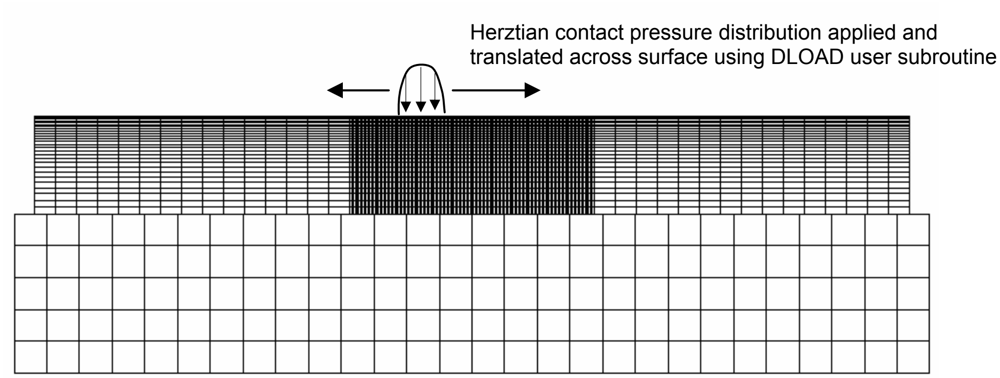

Figure 10. Simplified 'free' rolling contact model

Figure 11 shows the results obtained from this model for analyses with and without the NLGEOM option activated. It should be noted that the results now correspond to the softer 'plate' material properties and not those of the roller.

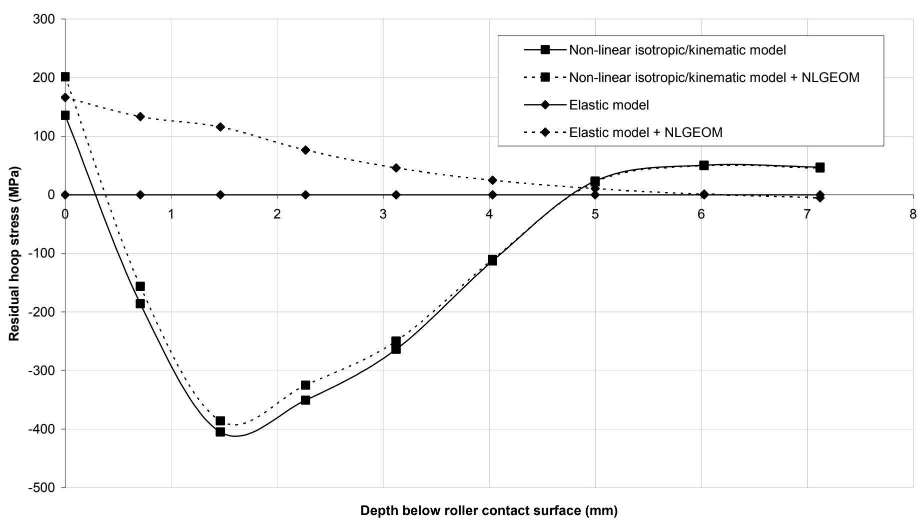

Figure 11. Effect of NLGEOM on results of simple rolling contact model

A clear difference can be observed between the geometrically linear and non-linear cases.

3.4 Discussion of Differences Between Predicted and Actual Residual Stress Distributions

Even when the spurious stress has been effectively removed from the model, the FEA results do not predict the large compressive stress at the surface of the roller observed in the experimental data shown in Figure 7. Surface compressive stresses can be generated by significant tangential as well as normal contact pressures, such as would be exhibited by tractive rolling. Although this has not been investigated in this instance, this aspect has been demonstrated in previous finite element analyses of rolling contact stresses (Jiang, Chang and Xu, 2001, Jiang, Xu and Sehitoglu, 2002, Guo and Barkey, 2004).

The 2D analysis predicted no sensitivity of the model behaviour to friction between the roller and plate for purely lateral plate motion. However, the actual setting of the bearings relative to the direction of local deck movement was such that it lead to skewed motion of the top plate and longitudinal sliding of the plate along the length of the roller. Guides attached to the upper and lower plates were also brought into contact with the end faces of the roller, leading to additional resistance to rolling and a greater tendency for the plates to slide. Both these factors have the potential to cause increased tangential force at the contact interface, although they have not been investigated in detail in this instance. In addition, the potential effects of surface roughness due to corrosion have also not been considered.

The analyses presented here could therefore be repeated in future work using a detailed 3D model to take into account these additional factors and improve the match of the FEA results to the experimental measurements. However, the number of cycles and mesh density required to perform this accurately would make this analysis computationally very expensive.

3.5 Review of Finite-Elastic, Finite-Plastic (FeFp) Material Model

A new material model has recently been developed by SIMULIA which may be used to remove the spurious stress observed in the analysis presented in this paper. The Finite-Elastic, Finite-Plastic (Fe-Fp) model corrects the elastic material model by using a total, as opposed to an updated, strain formulation in a similar way as hyperelastic materials, whilst also allowing the plastic behaviour of the material to be defined. However, it is understood that the model is currently restricted to use with isotropic hardening.

This model was unavailable within the current version of Abaqus at the time the analysis was performed, but has recently become available within the 'Extended Functionality' version of Abaqus released at the end of 2007. The analysis was therefore repeated by SIMULIA using the Fe-Fp model. The results of the Fe-Fp model are compared to those obtained from an equivalent model with isotropic hardening in Figure 12. Note that the material properties used in this study to illustrate the effect of the FeFp model are different to those used in the main analyses reported.

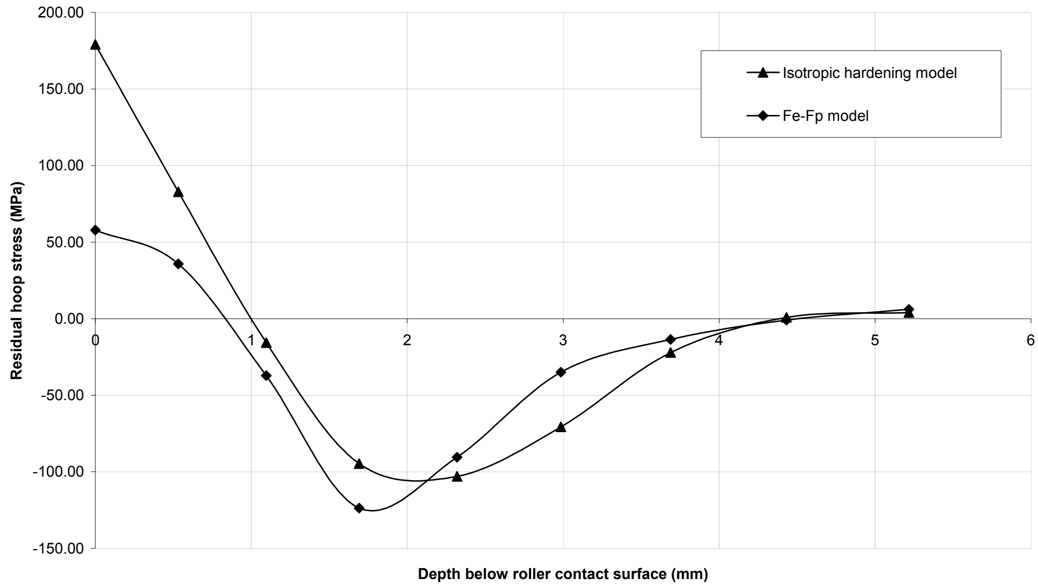

Figure 12. Comparison of residual stress predictions in the roller for the Fe-Fp and standard elastic plus isotropic hardening models

Figure 12 shows a clear difference in residual hoop stress predicted by the two models, with the Fe-Fp showing a reduced tensile stress at the roller surface. However, the main limitation of the Fe-Fp model is that it can only be used with isotropic hardening. It is therefore not considered appropriate for those simulations where the non-linear geometry (NLGEOM) option is required with kinematic and isotropic hardening of a material.

4. Conclusions

Predictions of the residual stresses in bridge roller bearings have been made using finite element analysis. Several material models have been investigated, of which the non-linear isotropic/kinematic hardening model has given the closed match to the results. However, in all cases a 'spurious' tensile residual stress has been observed at the roller surface that remains even for analyses using purely elastic material. This has been shown to be caused by numerical features.

When conducting an analysis involving cyclic plasticity and non-linear geometry, care must be taken to ensure the accuracy of the results is not affected by the updated strain formulation used by Abaqus. This issue may be overcome by ensuring a sufficiently small increment size is used in an analysis, however, for large models this may lead to increased computational expense.

Although the newly implemented Fe-Fp model corrects this problem, it can currently only be used with isotropic hardening, and is therefore not appropriate in instances where kinematic hardening is significant.

5. References

1. Konter, A., "How to Undertake a Contact and Friction Analysis," MARC Europe, NAFEMS Ltd, 2000.
2. Johnson, K.L., "Contact Mechanics," Cambridge University Press, 1987.
3. Jiang, Y., Chang, J., and Xu, B., "Elastic-Plastic Finite Element Analysis of Two-Dimensional Rolling Contact," Hydraulic Failure Analysis: Fluids, Components and Systems Effects, ASTM STP 1339, 2001.
4. Jiang, Y., Xu, B., and Sehitoglu, H., "Three-Dimensional Elastic-Plastic Stress Analysis of Rolling Contact," ASME Journal of Tribology, Volume 124, Part 4, pp 699-70, 2002.
5. Guo, Y. B., and Barkey, M.E., "FE-simulation of the effects of machining-induced residual stress profile on rolling contact of hard machined components," International Journal of Mechanical Sciences, Volume 46, 371-388, 2004.
6. Schindler, H. J., "Experimental determination of crack closure by the cut compliance method," ASTM STP 1343, R. McClung and J. C. Newman Eds., American Society for Testing and Materials, West Conshohocken, P. A., (1999), pp 175-187